Synthesis and electrical properties of lead-free piezoelectric Bi0.5Na0.5TiO3 thin films prepared by Sol-Gel method

Sara Abou Dargham, Freddy Ponchel, N. Abboud, M. Soueidan, Anthony Ferri, Rachel Desfeux, Jamal Assaad, Denis Remiens, Doumit Zaouk

Synthesis and Electrical properties of lead-free piezoelectric $Bi_{0.5}Na_{0.5}TiO_3$ thin films prepared by Sol-Gel method

S. Abou Dargham [a,b *], F. Ponchel [b], N. Abboud [a], M. Soueidan [c], A. Ferri [d], R. Desfeux [d], J. Assaad [b], D. Remiens [b], D. Zaouk [a]

a) Applied Physics Laboratory, Lebanese University, B.P 90656 Fanar, Lebanon
b) IEMN – DOAE – MIMM Team, UVHC – Le Mont Houy – 59313 – Valenciennes, France
c) Lebanese Atomic Energy Commission – CNRS, Riad l Solh, Lebanon
d) Université d'Artois, Unité de Catalyse et Chimie du Solide (UCCS) – 62300 – Lens, France

*** Sara.AbouDargham@etu.univ-valenciennes.fr**

Abstract: Lead-free $Bi_{0.5}Na_{0.5}TiO_3$ (BNT) piezoelectric thin films were deposited on $Pt/TiO_x/SiO_2/Si$ substrates by Sol-Gel method. A dense and well crystallized thin film with a perovskite phase was obtained by annealing the film at 700ºC in a rapid thermal processing system. The relative dielectric constant and loss tangent at 12 kHz, of BNT thin film with 350 nm thickness, were 425 and 0.07, respectively. Ferroelectric hysteresis measurements indicated a remnant polarization value of 9 $\mu C/cm^2$ and a coercive field of 90 kV/cm. Piezoelectric measurements at the macroscopic level were also performed: a piezoelectric coefficient ($d_{33effmax}$) of 47 pm/V at E = 190 kV/cm was obtained. The piezoresponse force microscopy data confirmed that BNT thin films present ferroelectric and piezoelectric behavior at the nanoscale level.

Keywords: Piezoelectric, Lead-Free, Sol-Gel, Thin Films, BNT.

Introduction

Piezoelectric materials play an important role in electronic and microelectronic systems (actuators, sensors, transducers, etc.) [1]. Lead-based compounds (such as PZT) are the most used materials due to their excellent piezoelectric properties. However, due to the effects of lead toxicity, it has recently desired to reduce lead-based materials usage in electronic devices [2]. Therefore, lead-free materials have a high interest recently in the microelectronic industry.

Bismuth sodium titanate $Bi_{0.5}Na_{0.5}TiO_3$, discovered by ***Smolenskii et al.*** in 1961 [3], is considered a good alternative lead-free material to PZT systems. BNT ceramics showed good ferroelectric properties: a strong remanent polarization $P_r = 30 – 38\ \mu C/cm^2$, and a high Curie temperature Tc ~ 320ºC [4, 5]. Relatively high piezoelectric coefficients ($d_{33} = 60 – 90$ pC/N) were reported for BNT ceramics [5, 6].

However pure BNT, especially in the form of thin film, suffers from large coercive field and high leakage current which make difficult to achieve successful poling**.** These disadvantages limit BNT system applications. Thus, to overcome these problems and to improve electrical properties, several approaches were adopted, such as composition modification of BNT [7, 8], multilayer structure [9] and orientation control [10]. In particular, the solid solution systems of BNT and $BaTiO_3$ (BT) show remarkable piezoelectric performance for composition close to the Morphotropic Phase Boundary (MPB) [4].

For BNT-BT thin films deposited on Pt/TiO_2/ SiO2/Si by chemical solution deposition (CSD), ***Alonso-Sanjose et al.*** demonstrated that an excess on the A-site (Na + Bi) improves electrical properties [11]. Furthermore, ***Pérez-Mezcua et al.*** investigated the crystallographic nature and the structural properties of BNT-BT thin films prepared by CSD with and without excesses of (Bi + Na) [12, 13]. They have also studied the electrical properties of these BNT-BT thin films [14], and obtained, for films without excesses,

the best piezoelectric properties in the region of MPB, while the films prepared with excess of Na or Bi presented a deformed piezoelectric response which could be related with the large conductivity and leakage currents.

However, up to now, few studies have focused on BNT thin films. Films were prepared by different methods: RF sputtering [15, 16], sol-gel [17 - 21], laser ablation [22 - 24]. Although growth parameters, dielectric and ferroelectric properties for BNT thin films were discussed, piezoelectric properties at the macroscopic scale were rarely investigated [16, 25].

In this paper, we present structural results obtained for BNT thin films prepared by Sol-Gel method on $Pt/TiO_x/SiO_2/Si$ substrate. Then, dielectric, ferroelectric and piezoelectric properties of these films were also investigated. Electrical characterizations of the films were carried at the local scale as well as at the macroscopic level.

Experimental procedure

BNT precursor was prepared by a modified nitrate–alkoxide sol–gel technique [20]. Bismuth III nitrate pentahydrate ($Bi(NO_3)_3.5H_2O$), sodium nitrate ($NaNO_3$) and titanium isopropoxide ($Ti(OC_3H_7)_4$) were used as starting materials, while acetic acid, distilled water, and acetylacetone were used as solvents. In order to prepare BNT solution, Bi:Na:Ti ratio of 1:1:2 was used with a 20 mol% excess of sodium nitrate (to compensate the loss of sodium during heat treatments). First, sodium nitrate and bismuth nitrate were dissolved in distilled water and acetic acid, respectively. The solution of nitrates was then mixed at 70ºC under magnetic stirring. Acetylacetone was added to titanium (IV) isopropoxide in order to prevent hydrolysis. Finally the solution of nitrates was mixed with stabilized titanium isopropoxide under magnetic stirring until a transparent and stable yellow precursor is obtained.

The films were deposited on $Pt/TiO_x/SiO_2/Si$ substrate by spin coating, at 3000 rpm for 20 s. Each layer was dried at 100ºC on a hot-plate, pyrolyzed at 200ºC to remove residual organic compounds and annealed by Rapid Thermal Processing (RTP), ramping at 25ºC/sec, at various temperatures in ambient air. 350 nm-thick BNT films were obtained after repeating the process for 6 times.

The crystalline structure of the prepared BNT film was examined using X-ray diffraction (XRD, Siemens D5000, Germany). The surface and cross-sectional morphologies were observed by scanning electronic microscope (SEM, Zeiss Ultra 55). LNO top electrodes (circular shape, diameter = 150 µm) were deposited on the films by magnetron sputtering and patterned by a photolithography liftoff process for the subsequent electrical measurements. Dielectric constant and loss tangent were measured at 10 kHz frequency, at room temperature, using a HP 4192A LCR – meter under ac voltage of 0.1 V. Ferroelectric properties at the macroscopic scale of BNT films were studied using an aixACCT TF 2000 analyzer (Germany). P-E loops were measured at a frequency of 1 kHz at room temperature. An atomic force microscope (AFM, Multimode, Nanoscope IIIa; Digital Instruments, Digital Instrument) was used to observe the surface topography and the local piezoelectric response of the BNT film.

In addition, piezoresponse force microscopy (PFM) was utilized to investigate local electromechanical activity by the measurement of the small displacement of the film induced by the converse piezoelectric. The measurement was achieved by applying a sequence of DC bias up to 10 V superimposed on an AC signal V_{ac} (1.5 V, 2 kHz) via the PFM tip directly on the film surface without the top electrodes. Platinum/iridium coated silicon tips-cantilevers ($k \approx 45$ N/m) were used to reduce the electrostatic force effects. “In-field” loops were recorded after each step of DC bias applied to film surface (V_{DC} max) while “remnant” loops were recorded when DC bias was stepped back to zero ($V_{DC} = 0$). To minimize the

electrostatic interaction between the tip and the surface, remnant loops for BNT films were recorded [26]. PFM loops were obtained by plotting the phase and the displacement as a function of the DC voltage.
Piezoelectric properties at the macroscopic level were studied using a system based on a laser Doppler vibrometer [27]. A home-made system was developed in our laboratory to measure the d_{33} piezoelectric coefficient by the single beam method. A detailed description of the measurement method was reported by ***R. Herdier et al.*** [27]. This method used in our laboratory means to minimize the substrate contribution using small top electrodes (maximum diameter of 150 µm) and fixing the sample on a glass slide (with glue). The sample is clamped on a support (in our case, glass substrate) using a thin film of adhesive (glue) with good mechanical coupling. To carry out the piezoelectric hysteresis loop measurements, a V_{ac} voltage of 1 Vmrs at the frequency of 12 kHz was applied to the film with a variable V_{DC} bias voltage.

Results and Discussions

The XRD patterns of BNT thin films prepared at different temperature by RTP are shown in figure 1. Films annealed at 650ºC showed a low crystallization of BNT while films annealed at 700ºC were completely crystallized with a polycrystalline structure without any preferred orientation or secondary phase.

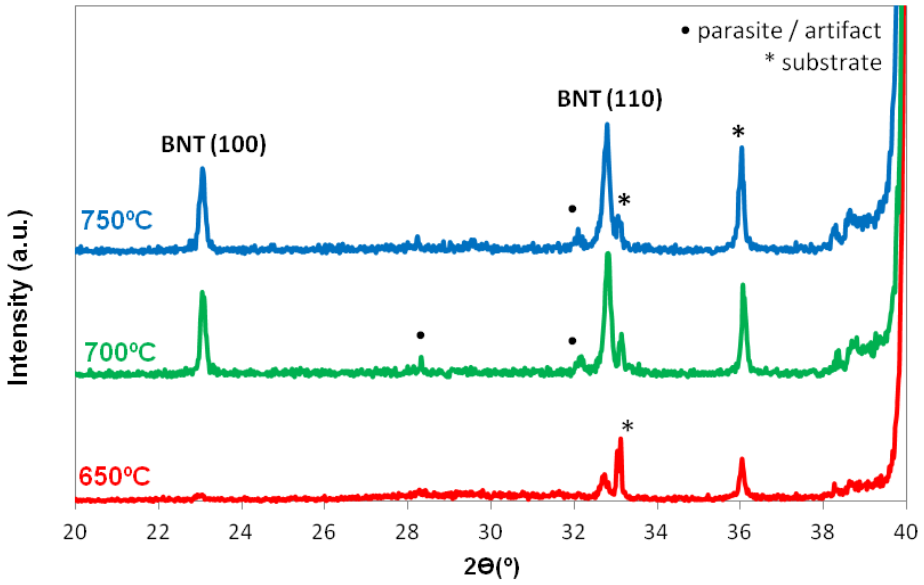

Figure 1 : XRD patterns of BNT thin films prepared by the rapid thermal process at different temperature in air.

Figure 2 shows SEM micrographs of BNT thin films (plan-view and cross-section images). BNT films annealed at 650 ºC (figure 2a – top) present few small intergrain pores on the surface, while films annealed at 700 ºC possess dense, uniform and crack-free micro-structure (figure 2b – top). Increasing the annealing temperature (figure 2c – top) cracks and pores were produced. The grains of BNT films are evenly distributed, and the grain size is about 100 nm. Thicknesses of these films were obtained from cross-sectional micrographs (figure 2 – bottom). BNT films show a uniform thickness of about 350 nm. The films annealed at 700ºC (figure 2b – bottom) exhibit a relatively dense and uniform grained structure, while the films annealed at 650ºC (figure 2b – bottom) present a heterogeneous structure with pores along the entire film thickness. However, for the films annealed at 750ºC (figure 2c – bottom), the lower layers (first layers) seem to be denser than the surface.

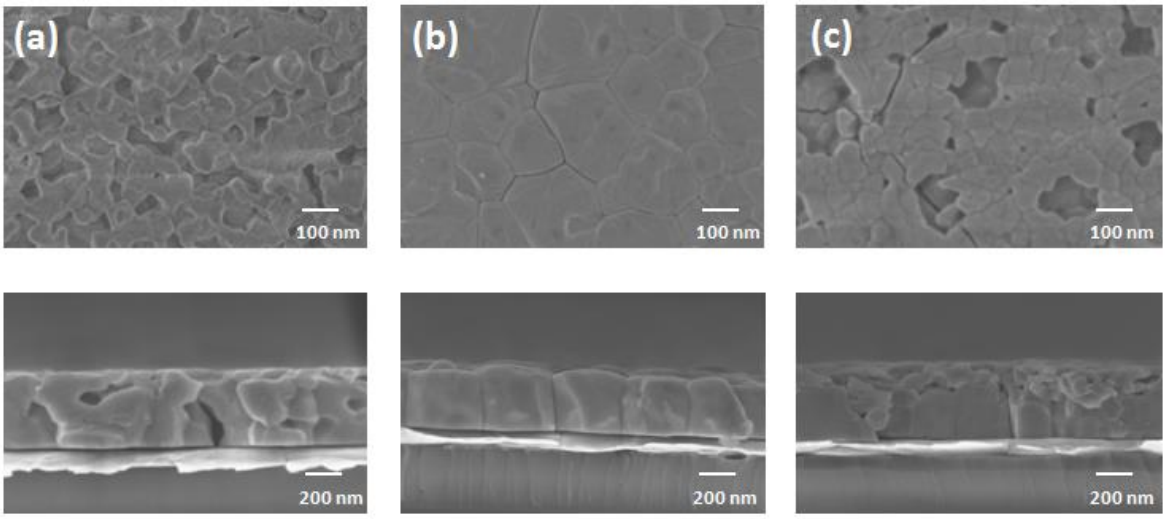

Figure 2 : Surface morphologies (at the top) and cross-sectional images (at the bottom) of BNT thin films annealed at (a) 650, (b) 700, (c) 750°C.

Raman spectroscopy of BNT thin film annealed at 700ºC with the RTP was recorded at room temperature. The deconvolution of the Raman spectrum shows six vibration modes for BNT situated at 109, 250, 502, 542, 778 and 861 cm^{-1}. Our results are close to the values reported in the literature for BNT thin films and ceramics [28 - 31].

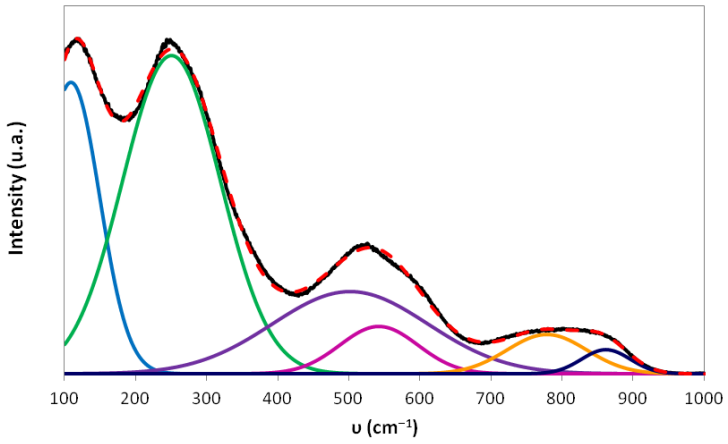

Figure 3 : Room temperature Raman spectrum for BNT thin film annealed at 700°C.

Figure 4 shows the voltage dependence of the dielectric properties for BNT thin films, calculated from the capacitance measured at room temperature and 12 kHz. Dielectric constant and loss tangent exhibit a significant change with the applied voltage with a hysteresis behavior typical for ferroelectric capacitors. Dielectric loops for BNT films annealed at different temperature are not centered at 0V; this shift could be attributed to different electrodes work function [32]. The maximum dielectric constant measured is about 425 for BNT films annealed at 700 and 750ºC while BNT film annealed at 650°C shows lower relative permittivity of 340. Our values are very close to dielectric constant values for BNT bulks (ε_r = 400). While for BNT thin films prepared by Sol-Gel, ***Yu et al.*** measured on a higher thickness (620 nm) a lower value of permittivity (ε_r = 277) [20].

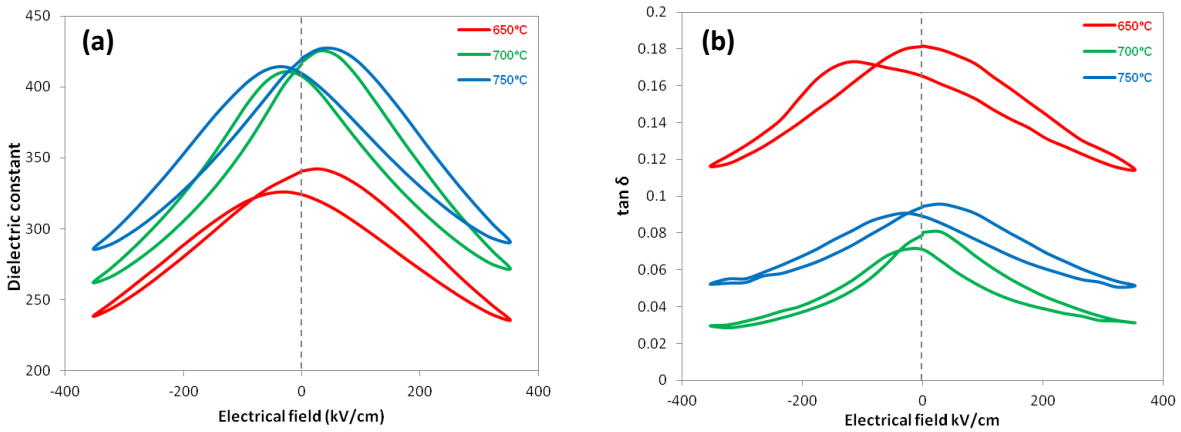

Figure 4 : Electrical field dependences of (a) the dielectric constant ϵ and (b) loss tan δ for the BNT thin films prepared in the RTP at different temperature.

BNT film annealed at 700ºC provides the minimum loss value (7%). However the 650ºC annealed film dielectric losses exhibit very significant value compared to the other samples (18%). The large dielectric loss can be attributed to the film microstructure. The denser microstructure was observed for the films annealed at 700 and 750 ºC, and hence these films show lower dielectric loss.

The ferroelectric properties of the BNT films were investigated by performing hysteresis measurements at a frequency of 1 kHz at room temperature. Figure 5 shows the P (E) loops of BNT thin films annealed at 650, 700 and 750°C. These hysteresis cycles prove the ferroelectricity of BNT films. The film annealed at 700 °C (figure 5b) presents a maximum value of the remnant polarization P_r = 9 µC/cm^2, the coercive electric field corresponding is E_c = 90 kV/cm for an applied voltage of 12 V. In fact, BNT films annealed at 700ºC have shown the best crystallinity (figure 1) and microstructure (figure 2a).

The loops are not fully saturated; for higher applied electric field, a rounded shape of the cycle is obtained (figure 5d). In addition, these P(E) loops are relatively slim and similar to those of classical relaxor-ferroelectrics PMN-PT films [33, 34], and this behavior of BNT-based thin films was reported by ***Perez-Rivero et al.*** [14]. The hysteresis loops show slight shifts on the vertical axis, this non-symmetry of the remnant polarization may be attributed to the asymmetry of the interfaces BNT / electrode**.** Such offset was reported in the literature for BNT-based thin films [14] [24]. Furthermore, the hysteresis loops are not located at zero voltage but shift slightly towards the positive voltage ($|Ec_{(+)}| > |Ec_{(-)}|$), which is coincident with the C(V) loops shown in Figure 4. This horizontal shift indicates that internal electric field produced by the electronic charges trapped near the interface ferroelectric film / bottom electrode [35]. Therefore, a positive larger field is required for domain switching.

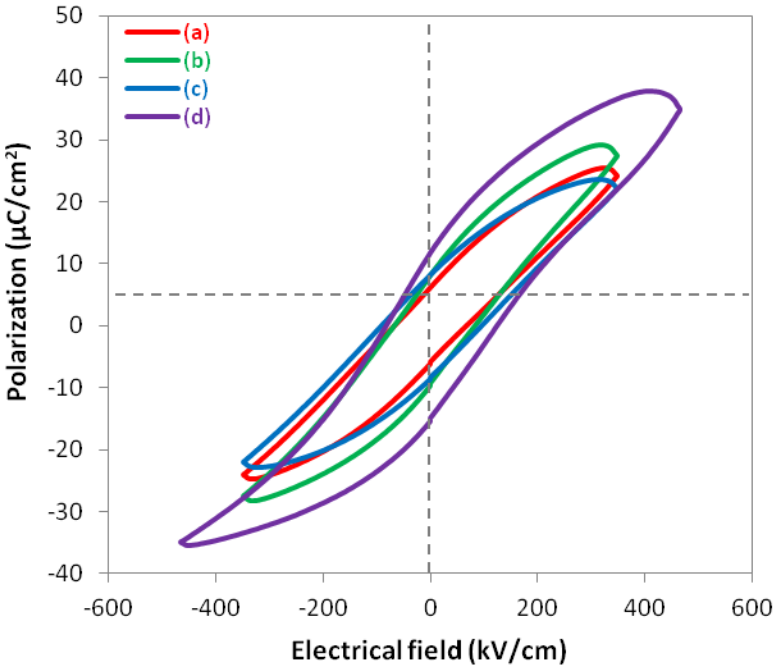

Figure 5 : Room temperature macroscopic ferroelectric hysteresis (P-E) loops of BNT thin films annealed at (a) 650°C, (b) 700°C, (c) 750°C, measured at 12 V, and (d) 700°C measured at 16 V.

Comparing our results to remnant polarization values typically reported in the literature, we notice that they are not too encouraging. Thus, to improve the ferroelectric performances, some optimizations will be introduced, such as annealing each layer in an oxygen atmosphere. It would be interesting to study the polarization retention (time-dependent polarization loss after poling), but from the shape of P(E) cycles and the relaxing character of BNT thin films, the retention should be very low. However the ferroelectric character of our material was demonstrated on the macroscopic scale.

Surface topography and PFM phase images of BNT films annealed at 700 °C are represented in figure 6. AFM topography image shows that BNT thin films exhibit a relatively dense grained structure and uniform grain size (Figure 6a). The PFM phase image (Figure 6b) shows that BNT film has a clear domain structure. The existence of strong and clear contrast regions indicates upward and downward polarized ferroelectric domains randomly distributed in BNT film.

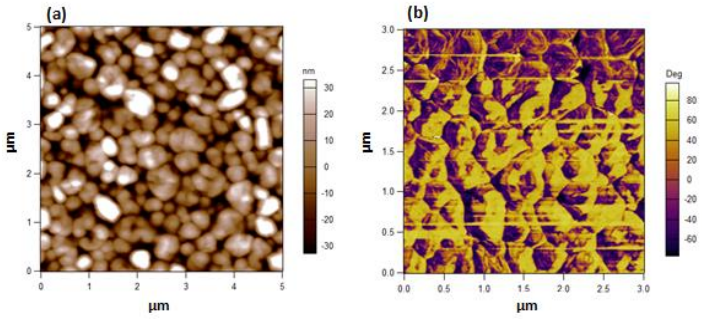

Figure 6 : (a) Morphology image and (b) piezoresponse image of BNT thin film.

Figure 7 shows typical phase-voltage hysteresis and amplitude-voltage butterfly loops. These measurements demonstrate the ferroelectric and piezoelectric behaviors of BNT films at the nanoscale level. The phase loop proves that domain switching was successfully achieved. The amplitude loop is asymmetric and shifted towards the positive voltage value which indicates the presence of a build-in electric field.

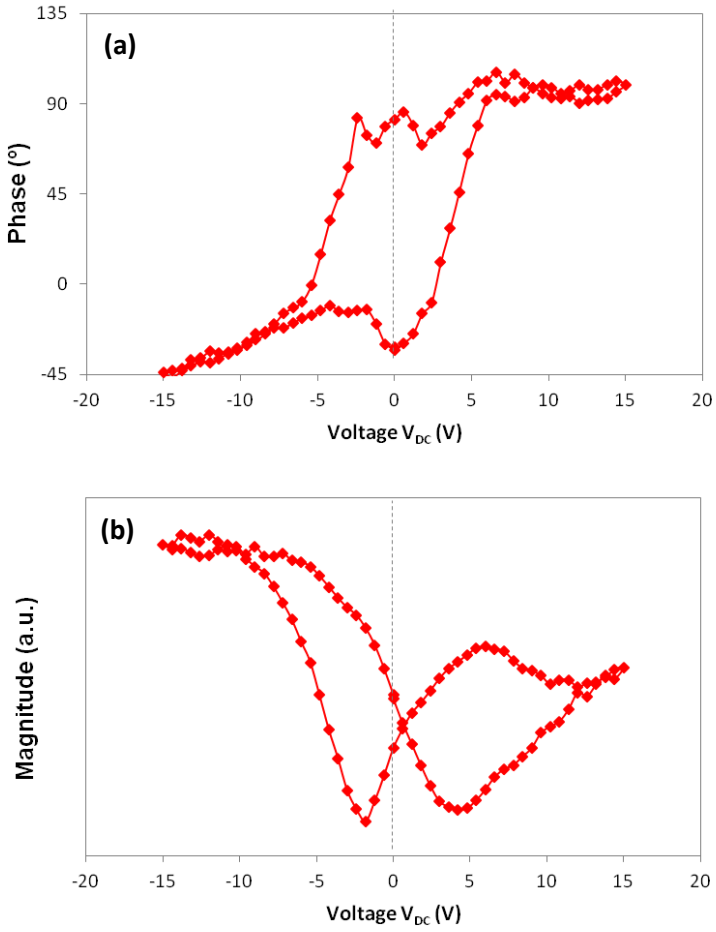

Figure 7 : Local piezoresponse (a) phase and (b) magnitude loops of BNT thin film measured at room temperature.

These measurements showed that the films exhibit an imprint reflecting blocking ferroelectric domains. This type of self-polarization was already demonstrated by PFM for BNT thin films prepared by PLD [23], as well as for PZT thin films obtained by sol-gel and sputtering [36, 37].

Figure 8 shows the $d_{33eff.}$ hysteresis loop of BNT films annealed at 700ºC. It can be seen that the film exhibits a typical ‘‘butterfly’’ loop. The maximum displacement, $d_{33eff.max}$ is 47 pm / V obtained at 190 kV / cm. Increasing the applied electrical field (beyond ± 8V) leads to the breakdown of our capacitors. Despite this effect, the d_{33} value is relatively important and shows the potential of BNT thin films to replace PZT thin films.

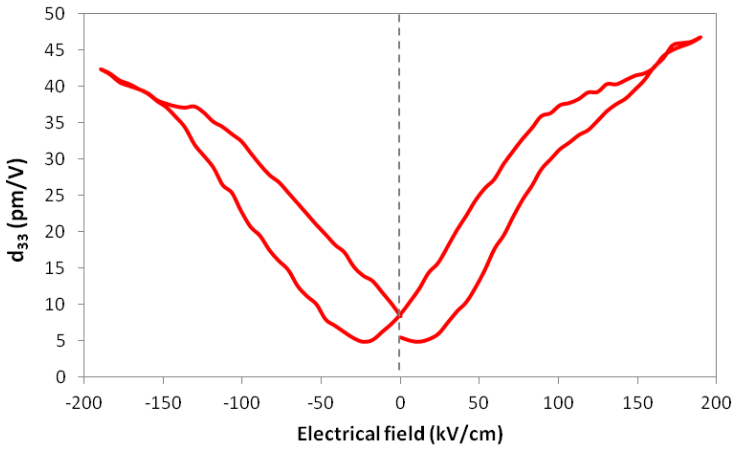

Figure 8 : d_{33}(E) loop of BNT film annealed at 700°C in the RTP.

Conclusion

Polycrystalline piezoelectric lead-free $Bi_{0.5}Na_{0.5}TiO_3$ (BNT) thin films (350 nm-thick) were grown on $Pt/Ti/SiO_2/Si$ substrates by sol–gel method. BNT films were crystallized into rhombohedral perovskite phase at 700 °C by rapid thermal processing. Resulting films are dense and present encouraging electrical properties. The dielectric constant and loss factor at a frequency of 12 kHz are 425 and 0.07, respectively. BNT films showed ferroelectric behavior at the macroscopic scale with difficulties to achieve the saturation of the P-E loop: remanent polarization (P_r) and coercive electric field (E_c) values are of 9µC/cm^2 and 90kV/cm, respectively. The existence of local piezoelectric and ferroelectric responses in BNT thin films was also demonstrated. Piezoelectric measurements at the macroscopic level were performed: a $d_{33effmax}$ coefficient of 47 pm/V was obtained. These results prove that BNT thin films prepared by Sol-Gel method present a promising lead-free candidate for microelectronic applications.

Acknowledgement

The authors gratefully acknowledge the Lebanese National Council for Scientific Research (CNRS-L) for financial support.

References

[1] B. Jaffe, W.R. Cook, H. Jaffe, Piezoelectric Ceramics, Academic, New York, 1971.
[2] E.-D. 2002/95/EC, Restriction of the Use of Certain Hazardous Substances in Electrical and Electronic Equipment (RoHS), Official Journal of the European Union, vol. 46, pp. 19–23, 2003.
[3] G.A. Smolenskii, A.I. Agranovskaya, Dielectric polarization of a number of complex compounds, Soviet Phys. Solid State 1 (10) (1960) 1429–1437.
4] T. Takenaka, K.-i. Maruyama, K. Sakata, (Bi1/2Na1/2)TiO3-BaTiO3 system for lead-free piezoelectric ceramics, Jpn. J. Appl. Phys. 30 (1991) 2236–2239.
[5] Q. Xu, X. Chen, W. Chen, S. Chen, B. Kim, J. Lee, Synthesis, ferroelectric and piezoelectric properties of some (Na0.5Bi0.5)TiO3, Mater. Lett. 59 (2005) 2437–2441.
[6] Y. Li, W. Chen, J. Zhou, Q. Xu, H. Sun, R. Xu, Dielectric and piezoelectric properties of lead-free (Na0.5Bi0.5)TiO3-NaNbO3 ceramics, Mater. Sci. Eng. B 112 (1) (2004) 5–9.
[7] T. Takenaka, H. Nagata, Current status and prospects of lead-free piezoelectric ceramics, J. Eur. Ceram. Soc. 25 (2005) 2693.

[8] Y. Hiruma, H. Nagata, T. Takenaka, Phase diagrams and electrical properties of (Bi1/2Na1/2)TiO3(Bi1/2Na1/2)TiO3-based solid solutions, J. Appl. Phys. 104 (2008).
[9] Y. Guo, M. Li, W. Zhao, D. Akai, K. Sawada, M. Ishida, M. Gu, Ferroelectric and pyroelectric properties of (Na0. 5Bi0. 5)TiO3?BaTiO3 based trilayered thin films, Thin Solid Films 517 (2974) (2009).
[10] T. Harigai, Y. Tanaka, H. Adachi, E. Fujii, Piezoelectric properties of lead-Free (Na,Bi)TiO3–BaTiO3 (001) epitaxial thin films around the morphotropic phase boundary, Appl. Phys. Exp. 3 (111501) (2010).
[11] D.A. Sanjosé, R. Jiménez, I. Bretos, M. Calzada, Lead-Free ferroelectric (Na1/2Bi1/2)TiO3–BaTiO3 thin films in the morphotropic phase boundary composition: solution processing and properties, J. Am. Ceram. Soc. 92 (10) (2009) 2218–2225.
[12] D. Pérez-Mezcua, R. Sirera, I. Bretos, J. Ricote, R. Jimenez, L. Fuentes-Cobas, R. Escobar-Galindo, D. Chateigner, M.L. Calzada, Morphotropic phase boundary in solution-derived (Bi0.5Na0.5)1-xBaxTiO3 thin films: part I crystalline structure and compositional depth profile, J. Am. Ceram. Soc. 97 (4) (2014) 1269–1275.
[13] D. Pérez-Mezcua, M. Calzada, I. Bretos, J. Ricote, R. Jiménez, L. Fuentes-Cobas, R. Escobar-Galindo, D. Chateigner, R. Sirera, Influence of excesses of volatile elements on structure and composition of solution derived lead-free (Bi0.50Na0.50)1xBaxTiO3 thin films, J. Eur. Ceram. Soc. 36 (2016) 89–100.
[14] A. Perez-Rivero, J. Ricote, I. Bretos, M.L. Calzada, J.P. Cruz, J.R. Fernandes, R. Jiménez, Morphotropic phase boundary in solution-derived (Bi0. 5Na0.5)1–xBaxTiO3 thin films: part II functional properties and phase stability, J. Am. Ceram. Soc. 97 (4) (2014) 1276–1282.
[15] Z.H. Zhou, J.M. Xue, W.Z. Li, J. Wang, H. Zhu, J.M. Miao, Ferroelectric and electrical behavior of (Na0.5Bi0.5) TiO3 thin films, Appl. Phys. Lett. 85 (5) (2016) 804–806.
[16] S. Quignon, C. Soyer, D. Remiens, Synthesis and electrical properties of sputtered (Na0.5Bi0.5)TiO3 thin films on silicon substrate, J. Am. Ceram. Soc. 95 (2012) 3180–3184.
[17] J.P. Mercurio, P. Marchet, Thin films of Na0.5Bi0.5TiO3 deposited by spin-coating, Integr. Ferroelectr. 61 (2004) 163–165.
[18] X.-G. Tang, J. Wang, X.-X. Wang, H.L.-W. Chan, Preparation and electrical properties of highly (111)-oriented (Na0.5Bi0.5)TiO3 thin films by a sol-gel process, Chem. Mater. 16 (25) (2004) 5293–5296.
[19] C.H. Yang, Z. Wang, Q.X. Li, J.H. Wang, Y.G. Yang, S.L. Gu, D.M. Yang, J.R. Han, Properties of Na0.5Bi0.5TiO3 ferroelectric films prepared by chemical solution decomposition, J. Cryst. Growth 284 (2005) 136–141.
[20] T. Yu, K.W. Kwok, H.L.W. Chan, Preparation and properties of sol–gel-derived Bi0. 5Na0. 5TiO3 lead-free ferroelectric thin film, Thin Solid Films 515 (2007) 3563–3566.
[21] F. Remondiere, B. Malic, ˇ M. Kosec, J.-P. Mercurio, Study of the crystallization pathway of Na0.5Bi0.5TiO3 thin films obtained by chemical solution deposition, J. Sol-Gel Sci. Technol. 46 (2) (2008) 117–125.
[22] J.-R. Duclère, C. Cibert, A. Boulle, V. Dorcet, P. Marchet, C. Champeaux, A. Catherinot, S. Députier, M. Guilloux-Viry, Lead-free Na0.5Bi0.5TiO3 ferroelectric thin films grown by Pulsed Laser Deposition on epitaxial platinum bottom electrodes, Thin Solid Films 517 (2) (2008) 592–597.
[23] M. Bousquet, J.-R. Duclère, B. Gautier, A. Boulle, A. Wu, S. Députier, D. Fasquelle, F. Rémondière, D. Albertini, C. Champeaux, P. Marchet, M. Guilloux-Viry, P. Vilarinho, Electrical properties of (110) epitaxial lead-free ferroelectric Na0.5Bi0.5TiO3 thin films grown by pulsed laser deposition: macroscopic and nanoscale data, J. Appl. Phys. 111 (2012).
[24] M. Bousquet, L. Batista, J.L. Dellis, A. Boulle, U. Rabe, O. Durand-Drouhin, Y. Gagou, L. Dupont, V. Viallet, A. Zeinert, S. Hirsekorn, N. Lemée, Structural and electrical properties of Bi0.5Na0.5 TiO3 based superlattices grown by pulsed laser deposition, J. Appl. Phys. 116 (2014).
[25] T. Yu, K.-W. Kwok, H. Chan, Sol-gel derived lead-free piezoelectric Bi1/2Nal/2TiO3 thin film for MEMS applications, 15th IEEE International Symposium on Applications of Ferroelectrics (2006).
[26] C. Harnagea, M. Alexe, D. Hesse, A. Pignolet, Contact resonances in voltage-modulated force microscopy, Appl. Phys. Lett. 83 (2) (2003) 338–340.
[27] R. Herdier, D. Jenkins, E. Dogheche, D. Remiens, M. Sulc, Laser Doppler vibrometry for evaluating the piezoelectric coefficient d 33 on thin film, Rev. Sci. Instrum. 77 (2006).
[28] M. Zannen, H. Khemakhem, A. Kabadou, M. Es-Souni, Structural, raman and electrical studies of 2 at.% Dy-doped NBT, J. Alloys Compd. 555 (2013) 56–61.
[29] M. Zannen, M. Dietze, H. Khemakhem, M. Es-Souni, Ferroelectric (Na1/2Bi1/2)TiO3 thin films showing photoluminescence properties, Appl. Phys. A 117 (2014) 1485–1490.
[30] J. Wang, Z. Zhou, J. Xue, Phase transition, ferroelectric behaviors and domain structures of (Na1/2Bi1/2)1-xTiPbxO3 thin films, Acta Mater. 54 (2006) 1691–1698.

[31] M.K. Niranjan, T. Karthik, S. Asthana, J. Pan, U.V. Waghmare, Theoretical and experimental investigation of Raman modes, ferroelectric and dielectric properties of relaxor Na0.5Bi0.5TiO3, J. Appl. Phys. 113 (2013).
[32] B.G. Chae, Y.S. Yang, S.H. Lee, M.S. Jang, S.J. Lee, S.H. Kim, W.S. Baek, S.C. Kwon, Comparative analysis for the crystalline and ferroelectric properties of Pb(Zr,Ti)O3 thin films deposited on metallic LaNiO3 and Pt electrodes, Thin Solid Films 410 (2002) 107–113.
[33] M. Detalle, A. Ferri, A.D. Costa, R. Desfeux, C. Soyer, D. Remiens, Nanoscale study by piezoresponse force microscopy of relaxor 0. 7Pb(Mg1/3Nb2/3)O3-0.3PbTiO3 and 0.9Pb(Mg1/3Nb2/3)O3-0. 1PbTiO3 thin films grown on platinum and LaNiO3 electrodes, Thin Solid Films 518 (2010) 4670.
[34] M. Alguero, J. Ricote, R. Jimenez, J. Carreaud, B. Dkhil, J.M. Kiat, J. Holc, M. Kosec, Size effect in morphotropic phase boundary Pb(Mg1/3Nb2/3)O3–PbTiO3, Applied Physics Letter 91 (2007) 112905.
[35] J. Xu, Y. Liu, R.L. Withers, F. Brink, H. Yang, M. Wang, Ferroelectric and non-linear dielectric characteristics of Bi0.5Na0.5TiO3Bi0.5Na0.5TiO3 thin films deposited via a metallorganic decomposition process, J. Appl. Phys. 104 (2008).
[36] A.L. Kholkin, K.G. Brooks, D.V. Taylor, S. Hiboux, N. Setter, Self-polarization effects in Pb(Zr,Ti)O3 thin films, Integr. Ferroelectr. 22 (1998) 525.
[37] A. Wu, P.M. Vilarinho, V.V. Shvartsman, G. Suchaneck, A.L. Kholkin, Domain populations in lead zirconate titanate thin films of different compositions via piezoresponse force microscopy, Nanotechnology 16 (11) (2005) 2597.